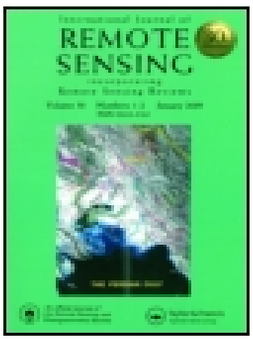

International Journal of Remote Sensing

ISSN: 0143-1161 (Print) 1366-5901 (Online) Journal homepage: http://www.tandfonline.com/loi/tres20

Development of circularly polarized synthetic aperture radar on-board UAV JX-1

J. Tetuko S. S., V.C. Koo, T. S. Lim, T. Kawai, T. Ebinuma, Y. Izumi, M. Z. Baharuddin, S. Gao & K. Ito

To cite this article: J. Tetuko S. S., V.C. Koo, T. S. Lim, T. Kawai, T. Ebinuma, Y. Izumi, M. Z. Baharuddin, S. Gao & K. Ito (2017): Development of circularly polarized synthetic aperture radar on-board UAV JX-1, International Journal of Remote Sensing

To link to this article: http://dx.doi.org/10.1080/01431161.2016.1275057

Published online: 13 Jan 2017.

Submit your article to this journal

View related articles

View Crossmark data

Full Terms & Conditions of access and use can be found at
http://www.tandfonline.com/action/journalInformation?journalCode=tres20

Download by: [218.33.149.117] **Date:** 13 January 2017, At: 06:30

INTERNATIONAL JOURNAL OF REMOTE SENSING, 2017
http://dx.doi.org/10.1080/01431161.2016.1275057

Taylor & Francis
Taylor & Francis Group

Development of circularly polarized synthetic aperture radar on-board UAV JX-1

J. Tetuko S. S.[a], V.C. Koo[b], T. S. Lim[b], T. Kawai[a], T. Ebinuma[c], Y. Izumi[a], M. Z. Baharuddin[a], S. Gao[d] and K. Ito[e]

[a]Centre for Environmental Remote Sensing, Chiba University, Chiba, Japan; [b]Faculty of Engineering and Technology, Multimedia University, Melaka, Malaysia; [c]Department of Electrics and Information, Engineering, Chubu University, Aichi, Japan; [d]School of Engineering and Digital Arts, University of Kent, Canterbury, UK; [e]Centre for Frontier Medical Engineering, Chiba University, Chiba-shi, Japan

ABSTRACT

We developed L band (frequency 1.275 GHz) circularly polarized synthetic aperture radar (circularly polarized SAR) on-board unmanned aerial vehicle (UAV). This paper explains the configuration of system, antenna, and car-based experiment of circularly polarized SAR. The comparison of circularly polarized SAR and linearly polarized SAR by full polarimetric scattering experiment in anechoic chamber was done and discussed. The result shows circular polarization has less effect of orientation angle of target and could avoid the misalignment of transmitter and receiver antenna during UAV operation. Axial ratio and ellipticity images are also derived and introduced as novel classification technique in microwave remote sensing field using circularly polarized SAR or ellipticity characteristic of scattering wave.

ARTICLE HISTORY
Received 31 July 2016
Accepted 8 December 2016

1. Introduction

Recently unmanned aerial vehicle (UAV) is implemented in remote sensing field for several applications (Aguasca et al. 2013; Alonso and Perez 2015; Bagheri 2016, Bi et al. 2016; Muraki and Ishikawa 2014, Yu et al. 2016). Josaphat Microwave Remote Sensing Laboratory (JMRSL) in Centre for Environmental Remote Sensing (CEReS), Chiba University, developed Josaphat Laboratory Experimental Unmanned Aerial Vehicle (UAV JX-1) to observe disaster and environmental change. This UAV JX-1 has 25 kg of payload and built for circularly polarized synthetic aperture radar (SAR) that works on L band (1.27 GHz, <150 MHz bandwidth), altitude 2000 m, output power 50 W (47 dBm), <1 m resolution, and total research budget about 1.2 million USD. This paper discusses the configuration of circularly polarized SAR system and antenna, including the result of car-based ground test and experiment of circularly polarized microwave scattering in anechoic chamber. Axial ratio and ellipticity images are also derived and introduced in this paper as novel classification technique in microwave remote sensing field using ellipticity characteristic of scattering wave of circularly polarized SAR.

CONTACT J. TETUKO S. S. jtetukoss@faculty.chiba-u.jp Centre for Environmental Remote Sensing, Chiba University, 1-33 Yayoi, Inage, Chiba 263-8522, Japan

© 2017 Informa UK Limited, trading as Taylor & Francis Group

2. Circularly polarized SAR

2.1. *Concept*

Figure 1(*a*) shows concept of the circularly polarized SAR for UAV. The antenna of circularly polarized SAR is installed on side (left or right) of UAV to illuminate the earth's surface by side looking configuration in strip-map observation mode. The transmitter (TX) transmits the left-handed circular polarization (LHCP) and right-handed circular polarization (RHCP). The transmitted L band microwave will be

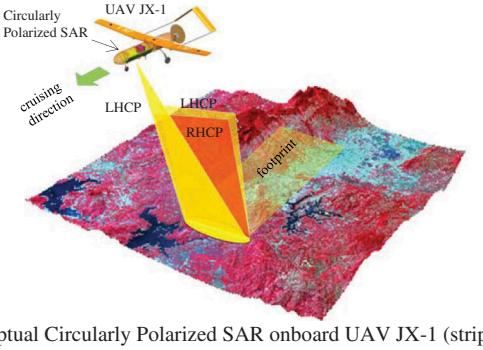

(*a*) Conceptual Circularly Polarized SAR onboard UAV JX-1 (stripmap mode)

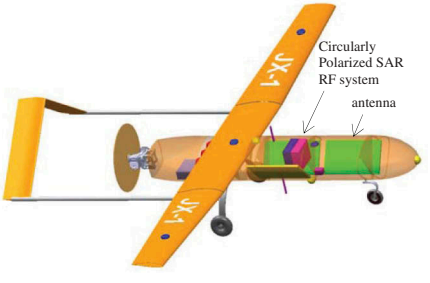

(*b*) Structure and payload of UAV JX-1

(*c*) Flying test of UAV JX-1

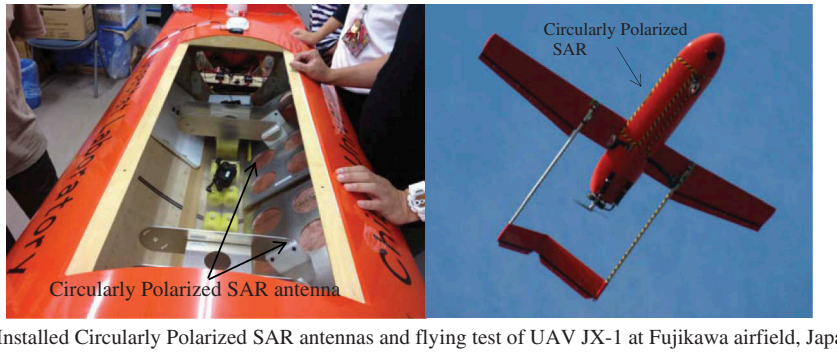

(*d*) Installed Circularly Polarized SAR antennas and flying test of UAV JX-1 at Fujikawa airfield, Japan

Figure 1. The concept of the UAV JX-1 mission and its experiment. (*a*) Conceptual circularly polarized SAR on-board UAV JX-1 (strip-map mode), (*b*) structure and payload of UAV JX-1, (*c*) flying test of UAV JX-1, (*d*) installed circularly polarized SAR antennas and flying test of UAV JX-1 at Fujikawa airfield, Japan.

scattered by the earth's surface and backscattered to the receiver's antenna on UAV. The value of intensity, polarization, and phase of scattered wave depends on structure, roughness, dielectric constant, or physical characteristics of object, etc. As shown in Figure 1(*a*), the scattered wave has LHCP and RCHP components, then receiver (RX) will receive these components simultaneously, and process the signal using range Doppler algorithm (RDA) to obtain raw data as in-phase signal (I or real data) and quadrature signal (Q or imaginary data). Then, we can process this image to acquire single-look complex (SLC) image, and further process to get the image of axial ratio, ellipticity, orientation angle of object, etc.

The circular polarization's mission has a benefit: circular polarization (CP) performs better than the HH (horizontal transmitting and horizontal receiving) polarization at lower incidence angles (Angelliaume et al. 2012). CP exhibits multiple benefits over linear polarization (LP) including avoiding polarization losses due to TX and RX antenna misalignment, where it also has the ability to reduce interference between direct and reflected signal due to multipath propagation (Touzi, Hurley, and Vachon 2015; Touzi and Vachon 2015). Design of circularly polarized SAR must be efficient on power consumption, where we must employ low nadir angle (about 20° to 30°) to reduce the transmitting power, particularly on mission of low frequency as L band.

Figure 1(*b*) shows the structure and position of installed circularly polarized SAR system, and antennas inside UAV JX-1, the details of specification and algorithm to calculate the parameter are explained in author's chapter in Nonami et al. (2013). The specifications of UAV JX-1 are shown in Table 1, where it is designed for operating at maximum altitude of 4000 m; cruising speed of 120 km h^{-1}; available antenna size of 0.4 m ° 1.5 m with off nadir angle of antenna beam being 20⁻60°, wing span 6 m, and length 4.75 m; maximum payload for sensor of 25 kg; and total weight of UAV of 146 kg.

Figure 1(*c*) shows UAV JX-1 operated by Chiba University for circularly polarized SAR mission, where detailed specifications of UAV JX-1 are calculated using author's algorithm in Nonami et al. (2013) and the result is shown in Table 1. Figures 1(*c*) and (*d*) show circularly polarized SAR antenna installed inside UAV and flying JX-1 UAV at Fujikawa Airfield, Japan.

Table 1. Specification of Josaphat laboratory experimental unmanned aerial vehicle (UAV JX-1).

Parameters	Values
Operating altitude	<4000 m
Off nadir angle of antenna beam	20–60°
Maximum size of antenna cargo	
Elevation	0.4 m
Azimuth	1.5 m
Beamwidth	
Elevation	<50°
Azimuth	<20°
Wing span	6 m
Length	4.75 m
Maximum payload (sensor)	25 kg
Total weight	146 kg

2.2. *Mission*

The main mission of the circularly polarized SAR is to hold basic research on elliptically polarized scattering and its application developments for disaster and environmental monitoring. In the basic research, we will investigate the scattering of elliptical polarization (EP) from the earth's surface to generate axial ratio, ellipticity, tilted angle images, etc., using characteristics of EP received by circularly polarized SAR. We will hold the analysis and experiment of CP of wave scattering on vegetation, snow, ice, soil, rock, sand, grass, etc., to investigate the characteristics of elliptical polarized scattering wave, including CP and LP. These images will be extracted by using the received RHCP and LHCP wave. Circularly polarized SAR transmits only one polarization (RHCP or LCHP), then this sensor will receive RHCP and LHCP scattering waves simultaneously, as shown in Figure 1(*a*). The received images (RHCP and LHCP) are then employed to investigate the relationship between the ellipticity characteristics and physical characteristics of vegetation, soils, snow, etc. Also the image of tilted angle as the response of land surface will be extracted to map the physical information of the surface, that is geological material, contour, snow–ice classification, vegetation characteristics, etc.

In application development, we plan to install this circularly polarized SAR on microsatellite GAIA-II that will be launched and implemented for disaster and environmental monitoring, that is land cover mapping, disaster monitoring, cryosphere monitoring, oceanographic monitoring, etc. Especially, land cover mapping will classify the forest and non-forest areas, estimate tree trunk heights, monitor mangrove areas and Arctic and Antarctic environment. In disaster monitoring, circularly polarized SAR will be employed for monitoring of earthquake area, volcano activity, landslides, etc.

2.3. *System*

As shown in Figure 2(*a*), the circularly polarized SAR system for UAV is mainly composed of signal generator or chirp pulse generator module, radio frequency (RF) system or TX and RX modules, and attitude controller, that is composed of inertial measurement unit (IMU) and GPS units. The input of TX is in phase (I) and quadrature (Q) signal of chirp pulse generated by pulse generator with baseband range is DC to 150 MHz (normally 50 MHz). As shown in Table 2, the chirp pulse is modulated by frequency 1270 MHz, where our TX–RX system has frequency range of 1270 ±50 MHz (maximum ±150 MHz). High power amplifier (HPA) is available to control pulse transmission output power to 50 W with pulse width maximum of 10 μs, and maximum duty circle of 2%. The antenna is composed of two sets of circularly polarized microstrip array antenna (LHCP and RHCP panels), totally four panels to realize full polarimetric circularly polarized SAR. We could control the pulse length and bandwidth of chirp pulse (maximum 150 MHz), and save data to SSD memory. Figures 2(*b*) and (*c*) show the RF system, chirp generator, and SAR image processor.

The specifications of circularly polarized SAR for UAV are as follows: centre frequency, 1270 MHz; ground resolution, up to 1 m; maximum pulse bandwidth, 150 MHz; available

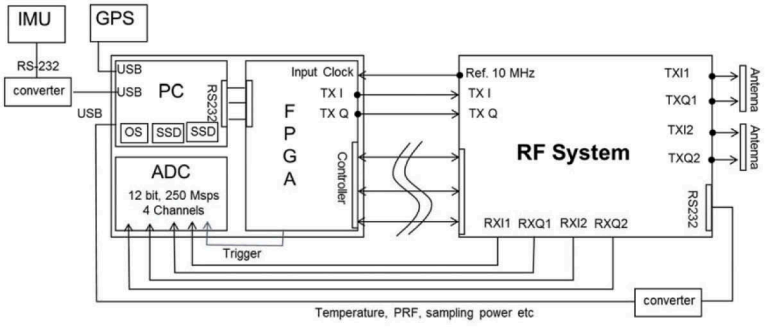

(*a*). Structure of Circularly Polarized SAR system

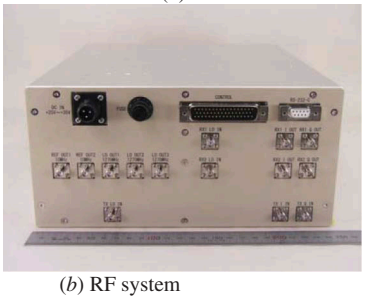

(*b*) RF system

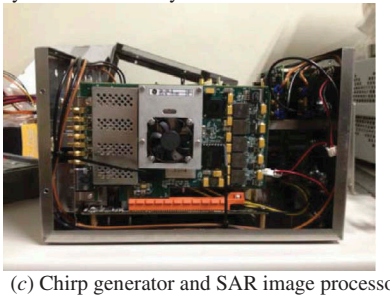

(*c*) Chirp generator and SAR image processor

Figure 2. (*a*) Structure, (*b*) RF system, (*c*) chirp generator and SAR image processor of circularly polarized SAR.

Table 2. Specification of circularly polarized SAR sensor for UAV JX-1.

Parameters	Values
Transmission frequency range	1270 ± 25 MHz (maximum 150 MHz)
Baseband range	DC to 50 MHz (maximum 150 MHz)
Pulse transmission output power	50 W (pulse width 10 μs (maximum), duty circle 2% (maximum))
Transmission system gain	+47 dB (minimum)
Receiver system gain	+60 dB (minimum)
Gain flatness	±1.5 dB (maximum)
Receiver noise ratio	3.5 dB (maximum) at 25°C
Modulator	(RX and TX) QPSK
Output higher harmonic wave	−30 dBc (maximum)
Output spurious	−60 dBc (maximum)
Transmission system gain tuning function	1/2/3/8/16 dB (0 to −31 dB)
Receiver system gain tuning function	1/2/3/8/16 dB x 2 (0 to −62 dB)
Impedance	50 W
Transmission system output VSWR	1.5:1
Receiver system input VSWR	1.5:1
Transmission system antenna switching speed	1 μs (typical)/2 μs (maximum)
Receiver system antenna switching speed	1 μs (typical)/2 μs (maximum)
Transmission system on/off speed	100 ns (maximum)
Receiver system on/off speed	100 ns (maximum)
Power voltage	DC +28 V (DC +25 to + 35 V switchable)
Current consumption	5 A (maximum)
Temperature	0–45°C
Saving temperature	−20 to 80°C
Weight	10 kg (maximum)
Size	W 250 mm × H 100 mm × D 300 mm

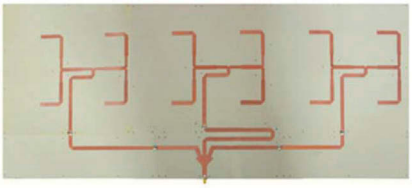

(*a*) Microstripline feeder

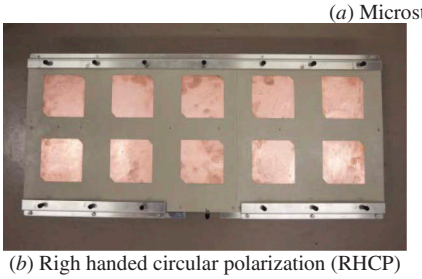

(*b*) Righ handed circular polarization (RHCP)

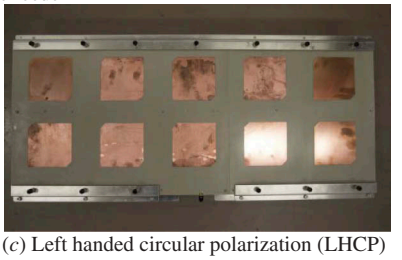

(*c*) Left handed circular polarization (LHCP)

Figure 3. Circularly polarized SAR antenna. (*a*) Microstripline feeder, (*b*) right-handed circular polarization (RHCP), (*c*) left-handed circular polarization (LHCP).

off nadir angle, 20–60°; swath width, 1 km; antenna size for four panels of circularly polarized SAR, 1.5 m ° 0.4 m; and pulse repetition frequency (PRF), 1000 Hz. We held ground experiment with altitude less than 2 km with pulse transmission output power 50 W. The data retrieved by LHCP and RHCP antenna, as shown in Figure 3, are developed and employed to investigate the characteristics of EP, including CP and LP.

3. Car-based experiment

Assessment of circularly polarized SAR system has been done by car-based experiment at study area along highway of Malaka, Malaysia, on 7 March 2015, as shown in Figure 4(*a*). By considering the safety of car-based experiment, we used two horn antenna as TX and RX and installed them on roof of the car. The pulse was transmitted with PRF 1000 Hz and car's velocity was 50 km h^{-1}. Trihedral corner reflector (width 1.5 m) was employed to validate and calibrate the scattering wave. SAR system illuminated the study area that comprised corner reflector side and two built-up business complexes (complex 1 and complex 2 in Figure 4(*a*)). Figure 4(*b*) shows the scattering image of our car-based L band SAR system that was processed using RDA to process the UAV SAR image signal processing. This figure shows that the corner reflector worked well. It also shows clear scattering and is used for validation of scattering image. The scattering from complex 1 and complex 2 also shows strong scattering, where this scattering is considered as reflection by metal inside the buildings. The skewed scattering is shown in the image; this effect is considered to be caused by the skewness of highway route as shown in Figure 4(*a*) that affects the processing of strip-map mode.

4. Experiment in anechoic chamber

The investigation of scattering of LP and CP has been done in this research by using N219 aircraft model as shown in Figure 5(*a*) by employing inverse SAR (ISAR) technique in our anechoic chamber. The objective of this research is to simulate scattering wave by

(a) Car based SAR and map of the study site

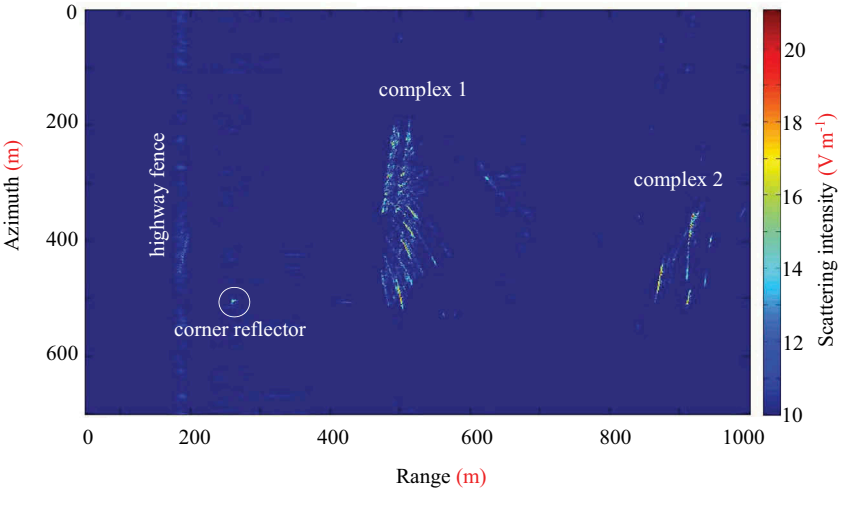

(b) Scattering image of study site

Figure 4. Car on-board SAR system test at Malaka, Malaysia. (*a*) Car-based SAR and map of the study site, (*b*) scattering image of study site.

employing circularly polarized SAR. We studied the scattering with various modes, for example horizontal transmitting and horizontal receiving (HH mode); horizontal transmitting and vertical receiving (VH mode); vertical transmitting and vertical receiving (VV mode); and vertical transmitting and horizontal receiving (HV mode) for linear polarization (LP mode). The circular polarization (CP mode) considered RHCP transmitting and RHCP receiving (RR mode), LHCP transmitting and RHCP receiving (RL mode), RHCP transmitting and LHCP receiving (LR mode), and LHCP transmitting and LHCP receiving (LL mode).

(*a*) Scattering target used N219 aircraft model

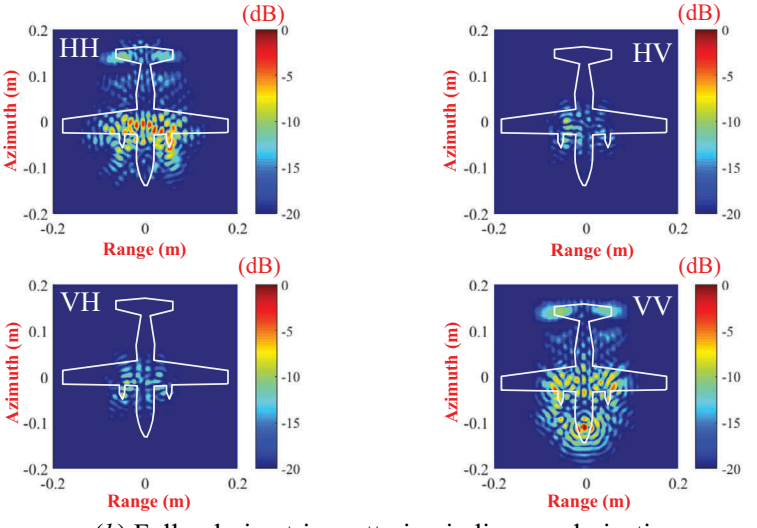

(*b*) Full polarimetric scattering in linear polarization

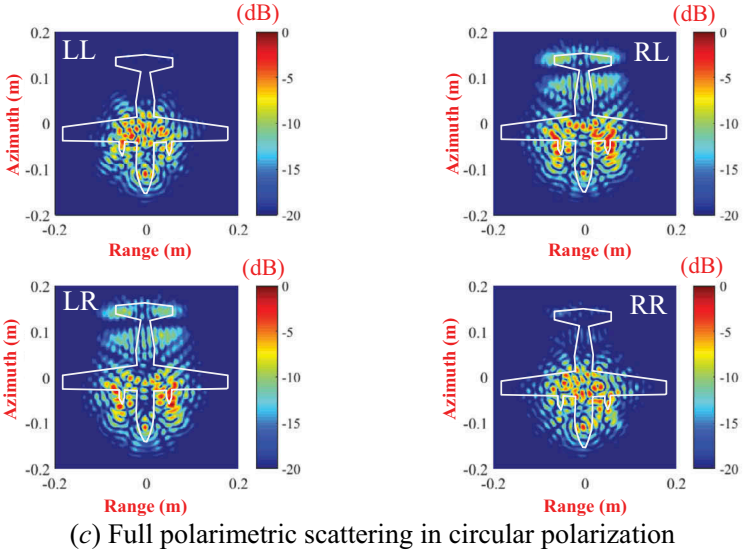

(*c*) Full polarimetric scattering in circular polarization

Figure 5. Circularly polarized scattering experiment. (*a*) Scattering target using N219 aircraft model, (*b*) full polarimetric scattering in linear polarization, (*c*) full polarimetric scattering in circular polarization.

Figure 5(*b*) shows that LP depicts co-polarization (HH and VV modes) which has strong scattering, whereas cross-polarization (HV and VH modes) has weak scattering. Cross-polarization shows volume scattering, and co-polarization shows surface scattering and double bounce (Migliaccio et al. 2011). It matches well with the full polarization theory (Yamaguchi 2007). This figure shows that LP has weak scattering than cross-polarization or volume scattering, especially scattering by main body of object. The co-polarization or surface scattering and double bounce shows strong intensity of scattering from main body, main wing, nose, tail, and propeller.

Figure 5(*c*) shows that CP has strong scattering from the main body of model on both co-polarization (LL and RR) and cross-polarization (LR and RL), but different scattering from tail. Co-polarization shows even-scattering (double bounce), and cross-polarization shows odd-scattering (surface scattering). It means that CP could avoid the effect of antenna misalignment and orientation angle of the antenna when installed on the side body of platform (UAV and aircraft); especially circularly polarized SAR could reduce the effect of air drag and platform's attitude during the observation using UAV.

Figure 6 shows images of ellipticity and axial ratio of circular polarized scattering of N210 aircraft model from Figure 5(*c*). The ellipticity ε (unit: radian) in Figure 6(*a*) is calculated by using intensity of LHCP and RHCP of scattering wave (E_L and E_R) as

$$\varepsilon = \frac{1}{2}\sin^{-1}\left\{\frac{|E_L|^2 - |E_R|^2}{|E_L|^2 + |E_R|^2}\right\}. \tag{1}$$

Zero radian of ellipticity means LP, positive value (0–0.25π) means LHCP, and negative value (–0.25π–0) means RHCP. Figure 6(*a*) shows that LHCP scattering wave occurred from tail wing and propellers. The main body scattered RHCP wave. We can use this information to classify the structure of targeted object as shown in this result.

Figure 6(*b*) shows axial ratio (AR) image which is calculated using

$$\mathrm{AR} = 20\ \log_{10}|\cot\varepsilon|, \tag{2}$$

with input of ellipticity ε shown in Figure 6(*a*). Zero value of ε means perfectly CP. We define EP for ellipticity from 0 to 20 dB, and LP for ellipticity with value more than 20 dB. This figure shows various values of EP of scattering wave from some parts of model, where main body has low value and tail has high scattering close to LP. This result shows the axial ratio and ellipticity could be employed to classify the object characteristics, that is shape, roughness, thickness, height, etc., by using circularly polarized SAR.

5. Conclusion

We developed circularly polarized SAR on-board UAV JX-1. This paper explained the system structure and performance of circularly polarized SAR. The result of car-based experiment of SAR shows the scattering image for SAR system. The comparison of LP and CP by microwave scattering experiment inside anechoic chamber was discussed, where the results show that CP affects less on orientation angle of target and could avoid the effect of TX and RX antenna misalignment. We plan to hold flight test of circularly polarized SAR system using UAV JX-1 and small aircraft for further investigation of circularly polarized SAR.

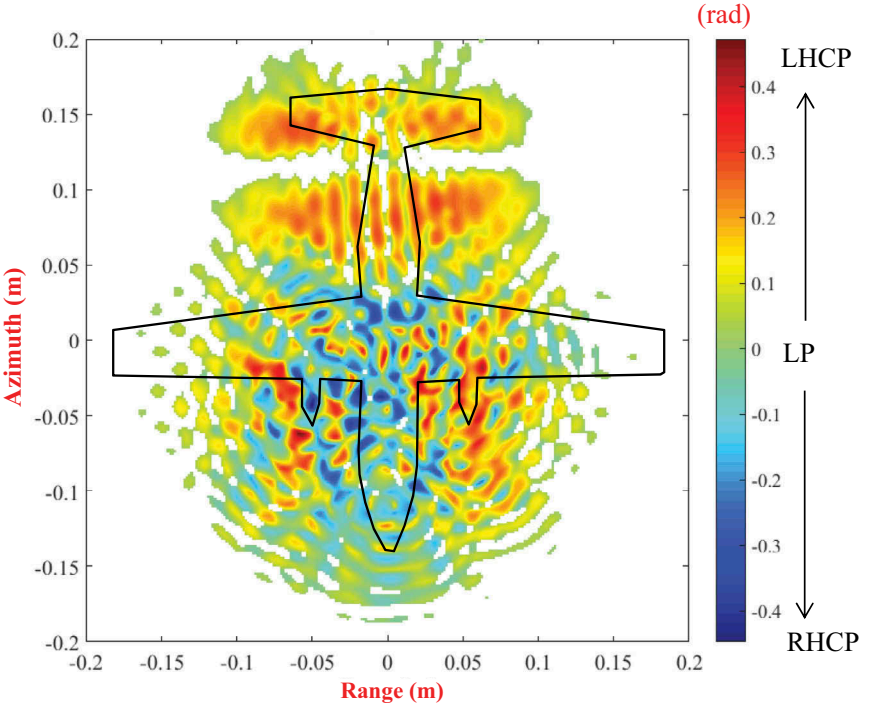

(*a*) Ellipticity

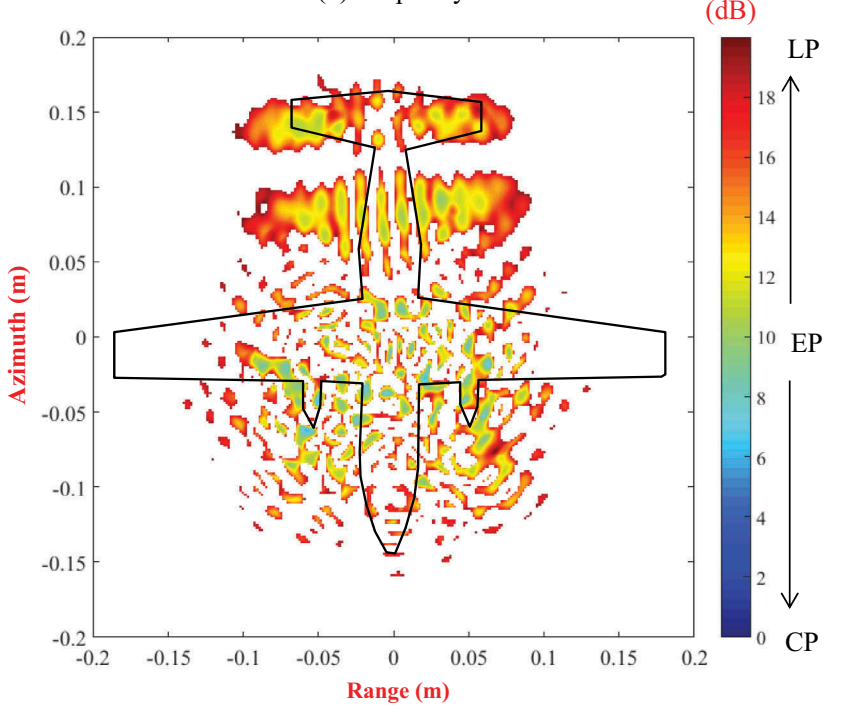

(*b*) Axial ratio

Figure 6. Axial ratio and ellipticity images of circular polarized scattering of N219 aircraft model (*a*) Ellipticity and (*b*) axial ratio.

Acknowledgements

This work was supported in part by the Japan Science and Technology Agency (JST) – Japan International Cooperation Agency (JICA) (FY2010–2016); Science and Technology Research Partnership for Sustainable Development (SATREPS)-Research and Development for Reducing Geo-Hazard Damage in Malaysia caused by Landslide and Flood; the European Space Agency's (ESA) Earth Observation Category 1 [grant number 6613]; the 4th Japan Aerospace Exploration Agency (JAXA) ALOS Research Announcement [grant number 1024]; the 6th JAXA ALOS Research Announcement [grant number 3170]; the Japanese Government National Budget – Ministry of Education and Technology (MEXT) (FY2015–2017) [grant number 2101]; Chiba University Strategic Priority Research Promotion Program, Chiba University Institute of Global Prominent Research [grant Chibagukidai 26]; Taiwan National Space Organization (NSPO) [grant number NSPIO-S-105096]; and Indonesian National Institute of Aeronautics and Space (LAPAN) LAPAN-A4/Lapan-Chibasat Project [grant number J09KF00807].

Disclosure statement

No potential conflict of interest was reported by the authors.

Funding

This work was supported in part by the Japan Science and Technology Agency (JST) – Japan International Cooperation Agency (JICA) (FY2010–2016); Science and Technology Research Partnership for Sustainable Development (SATREPS)-Research and Development for Reducing Geo-Hazard Damage in Malaysia caused by Landslide and Flood; the European Space Agency's (ESA) Earth Observation Category 1 under [Grant 6613]; the 4th Japan Aerospace Exploration Agency (JAXA) ALOS Research Announcement under [Grant 1024]; the 6th JAXA ALOS Research Announcement under [Grant 3170]; the Japanese Government National Budget – Ministry of Education and Technology (MEXT) (FY2015–2017) under [Grant 2101]; Chiba University Strategic Priority Research Promotion Program, Chiba University Institute of Global Prominent Research under [Grant Chibagukidai 26]; Taiwan National Space Organization (NSPO) under [Grant NSPIO-S-105096]; and Indonesian National Institute of Aeronautics and Space (LAPAN) LAPAN-A4/Lapan-Chibasat Project under [Grant J09KF00807].

References

Aguasca, A., R. Acevo, A. Broquetas, and X. Fabregas. 2013. "ARBRES: Light-Weight CW/FM SAR Sensors for Small Uavs." *Sensors* 13 (3): 3204–3216. doi:10.3390/s130303204.

Alonso, J. M. I., and M. S. Perez. 2015. "Phased Array for UAV Communications at 5.5 Ghz." *IEEE Antennas and Wireless Propagation Letters* 14: 771–774. doi:10.1109/LAWP.2014.2379442.

Angelliaume, S., P. Martineau, P. Durand, and T. Cussac. 2012. "Ship Detection and Sea Clutter Characterisation Using X & L Band Full Polarimetric Airborne SAR Data." *Proceedings of SeaSAR, Tromsø, Norway*, June 18-22, 709: 1–4.

Bagheri, N. 2016. "Development of a High-Resolution Aerial Remote-Sensing System for Precision Agriculture." *International Journal of Remote Sensing* 1–13. doi:10.1080/01431161.2016.1225182.

Bi, H., W. Zheng, Z. Ren, J. Zeng, and J. Yu. 2016. "Using an Unmanned Aerial Vehicle for Topography Mapping of the Fault Zone Based on Structure from Motion Photogrammetry." *International Journal of Remote Sensing* 1–16. doi:10.1080/01431161.2016.1249308.

Migliaccio, M., F. Nunziata, A. Montuori, and C. E. Brown. 2011. "Marine Added-Value Products by RADARSAT-2 Fine Quad-Polarization." *Canadian Journal of Remote Sensing* 37 (5): 443–451. doi:10.5589/m11-054.

Muraki, H., and N. Ishikawa. 2014. "Current State of the Unmanned Systems that Advance in Europe, United States, and Japanese Situation." *Japan Society of Photogrammetry and Remote Sensing* 53 (3): 123–127. doi:10.4287/jsprs.53.123.

Nonami, K., M. Kartidjo, K. J. Yoon, and A. Budiyono, eds. 2013. "Autonomous Control Systems and Vehicles: Intelligent Unmanned Systems." J. TETUKO S.S., Chap. 12 in *Circularly Polarized Synthetic Aperture Radar Onboard Unmanned Aerial Vehicle*. Tokyo: Springer.

Touzi, R., J. Hurley, and P. W. Vachon. 2015. "Optimization of the Degree of Polarization for Enhanced Ship Detection Using Polarimetric RADARSAT-2." *IEEE Transactions on Geoscience and Remote Sensing* 53 (10): 5403–5424. doi:10.1109/TGRS.2015.2422134.

Touzi, R., and P. W. Vachon. 2015. "RCM Polarimetric SAR for Enhanced Ship Detection and Classification." *Canadian Journal of Remote Sensing* 41 (5): 473–484. doi:10.1080/07038992.2015.1110010.

Yamaguchi, Y. 2007. *Radar Polarimetry: Basic and Application – Radar Remote Sensing Using Polarimetry*. Tokyo: IEICE.

Yu, X., Q. Liu, X. Liu, X. Liu, and Y. Wang. 2016. "A Physical-Based Atmospheric Correction Algorithm of Unmanned Aerial Vehicles Images and Its Utility Analysis." *International Journal of Remote Sensing* 1–12. doi:10.1080/01431161.2016.1230291